



Nickel utilization in phytoplankton assemblages from contrasting oceanic regimes

Christopher L. Dupont^{a,*}, Kristen N. Buck^{b,2}, Brian Palenik^c, Katherine Barbeau^b

^a Scripps Institution of Oceanography, University of California, San Diego, La Jolla, CA 92093, USA

^b Geosciences Research Division, Scripps Institution of Oceanography, University of California, San Diego, La Jolla, CA 92093, USA

^c Marine Biology Research Division, Scripps Institution of Oceanography, University of California, San Diego, La Jolla, CA 92093, USA

ARTICLE INFO

Article history:

Received 10 May 2009

Received in revised form

23 December 2009

Accepted 7 January 2010

Available online 28 January 2010

Keywords:

Nickel

Iron

Phytoplankton

Uptake kinetics

Colimitation

ABSTRACT

In most oceanic environments, dissolved nickel (Ni) concentrations are drawn down in surface waters with increasing concentrations at depth, implying a role for biology in the geochemical distribution of Ni. Studies with phytoplankton isolates from the surface ocean have established the biochemical roles of Ni in the assimilation of urea and oxidative defense. To determine if these requirements are relevant in natural marine planktonic assemblages, bottle-based fertilization experiments were used to test the effects of low-level additions of Ni, urea, or both Ni and urea to surface waters at several locations offshore of Peru and California, as well as in the Gulf of California. Urea and Ni+urea additions consistently promoted phytoplankton growth relative to control and +Ni treatments, except in a coastal upwelling site and Peruvian water. No effect was observed in the upwelling site, but in Peruvian waters urea additions resulted in increased phytoplankton pigments and phosphate drawdown only when Ni was added concurrently, suggesting a biochemically dependent Ni–urea colimitation. In the Gulf of California, Ni additions without urea resulted in increased abundances of cyanobacteria, picoeukaryotes, and the corresponding pigments. As urea additions showed the overall phytoplankton community was also urea-limited, it appears that the cyanobacteria and potentially the picoeukaryotes were colimited by Ni and urea in a biochemically independent fashion. In parallel, radiotracer-based uptake experiments were used to study the kinetics and spatial variation of biological Ni assimilation. In these experiments, the added radiotracer rarely equilibrated with the natural Ni present, precluding estimates a determination of *in situ* Ni uptake rates and suggesting that much of the natural Ni was not bioavailable. The lack of equilibration likely did not preclude the measurement of community Ni uptake kinetics, nor the comparison of measured rates between locations. The highest $V_{\max}K_p^{-1}$ values, which reflect a competitive advantage in Ni acquisition at low concentrations, were observed in stratified nitrogen-deplete communities, potentially linking Ni and nitrogen biogeochemistry in a manner consistent with the biochemical utilization of Ni. Overall, uptake rates were higher in the euphotic rather than non-euphotic zone communities, directly reconciling the nutrient-like depth profile of Ni. The Ni uptake rates observed at the nitrate-replete Fe-deplete Peru stations were an order of magnitude lower than the other sites. This result agrees with calculations suggesting that saturation of the cell surface with Ni and iron (Fe) transporters may limit uptake rates in low Fe waters.

© 2010 Elsevier Ltd. All rights reserved.

1. Introduction

The dissolved concentrations of many of the elements or compounds required by marine phytoplankton are drawn down to a minimum in the surface ocean and increase with depth, a gradient denoted as “nutrient-like.” The underlying mechanisms behind these gradients are the assimilation of dissolved nutrients

by primarily photosynthetic prokaryotes and eukaryotes in the sunlit surface, and remineralization of sinking biomass by heterotrophic microbes. The “nutrient-like” depth profile of dissolved nickel (Ni) in seawater was noted in 1976, as was the strong correlation in the dissolved concentrations of Ni and the macronutrients H_4SiO_4 and PO_4^{3-} (Sclater et al., 1976). At the time, no biological need for Ni in marine phytoplankton had been identified.

Over the past 30 years, culture and genomic studies have identified two widespread biological requirements for Ni in marine phytoplankton. Ni functions as an essential cofactor in both urease and Ni–superoxide dismutase, which influences an organism’s Ni requirements. Most marine phytoplankton,

* Corresponding author. Tel.: +1 858 200 1886; fax: +1 858 200 1881.

E-mail address: cdupont@jcvl.org (C.L. Dupont).

¹ Current address: J. Craig Venter Institute, San Diego, CA 92121, USA.

² Current address: Bermuda Institute of Ocean Sciences, St. George’s GE 01, Bermuda.

including cyanobacteria (Collier et al., 1999), coccolithophores (Palenik and Henson, 1997), dinoflagellates (Dyhrman and Anderson, 2003), cryptophytes, chrysophytes, and prasinophytes (Oliveria and Antia, 1986), use the Ni-containing enzyme urease to hydrolyze urea to ammonium and carbon dioxide. Consequently, these phytoplankton require Ni to grow on urea, an ecologically important reduced nitrogen source that can support 5–50% of oceanic primary production (Wafar et al., 1995). When a urease-utilizing phytoplankton growing on urea as a nitrogen source is deprived of Ni, growth will cease due to a biochemically dependent Ni–Nitrogen colimitation (Dupont et al., 2008a; Price and Morel, 1991). In this scenario, the addition of either Ni, which results in a functional urease, or a nitrogen source like NH_4^+ or NO_3^- , which do not require Ni for assimilation, will restore growth. Some phytoplankton of the green lineage, including *Chlamydomonas* and *Chlorella*, can cleave urea using the non-Ni containing enzyme urea-amidolyase (Hausinger, 2004), though these organisms are not believed to be prevalent in the marine environment.

The harmful oxygen species superoxide, generated circumstantially by electron transport chains in the presence of oxygen, is reduced and oxidized to molecular oxygen and hydrogen peroxide by superoxide dismutases (SOD, Fridovich, 1997). The importance of SOD in oxidative defense is such that a functional SOD is essential for growth in aerobic organisms. Ni-containing SOD, a recently discovered isoform of superoxide dismutase, is evolutionarily and structurally distinct from the Fe, Mn, and Cu-containing isoforms of SOD (Barondeau et al., 2004). The gene coding for Ni–SOD, *sodN*, is found in the genomes of most marine cyanobacteria, including *Synechococcus*, *Prochlorococcus*, *Trichodesmium*, and *Crocospaera*, the cosmopolitan picoeukaryote *Ostreococcus*, and an array of heterotrophic bacteria (Dupont et al., 2008b). *Synechococcus* strains with a Ni–SOD have an obligate need for Ni to maintain maximal growth rates irrespective of nitrogen source, with Ni deprivation resulting in reduced cellular superoxide dismutase activity and eventually cessation of growth (Dupont et al., 2008a). This physiological result, when coupled with comparative genomics, suggests that most marine *Synechococcus* and all *Prochlorococcus* have an obligate Ni requirement (Dupont et al., 2008a). Genomic analyses also show that the acquisition of the gene coding for Ni–SOD involved a direct replacement of a gene coding for Fe–SOD, implying an evolutionary tradeoff between Ni and Fe requirements (Dupont et al., 2008b).

Two of the aforementioned culture studies also examined Ni uptake rates as a function of extracellular Ni concentrations and the nitrogen source for growth in diatoms (Price and Morel, 1991) and cyanobacteria (Dupont et al., 2008a). In both studies, reduced extracellular and intracellular Ni concentrations prompted increased maximal uptake rates, but this response was modulated by the nitrogen source for growth. The diatom *Thalassiosira weissflogii* only accumulated Ni when growing on urea, otherwise eschewing the element (Price and Morel, 1991). In contrast, *Synechococcus* WH8102 and CC9311, requiring Ni for both urease and Ni–SOD, actively took up Ni when growing on NH_4^+ , urea, and NO_3^- , though the highest uptake rates were observed for growth on urea (Dupont et al., 2008a). These results imply that Ni cycling in the ocean depends upon both phytoplankton community composition and nitrogen biogeochemistry. As an extreme example, nitrate-rich, diatom-dominated communities traditionally found in upwelled waters would be expected to have lower biomass-normalized Ni uptake rates compared with cyanobacteria communities growing on recycled nitrogen sources like urea and NH_4^+ , a scenario common to stratified oligotrophic waters. To date, Ni uptake rates and kinetics have not been studied in oceanic communities.

From these culture studies, it follows that certain phytoplankton can be directly limited by low Ni if they depend upon Ni–SOD. Biochemically dependent Ni–urea colimitation is also possible, where urease-catalyzed urea assimilation is limited by low Ni concentrations (Saito et al., 2008). Given the paucity of Ni-independent urea assimilation pathways, it seems likely that such Ni–urea colimitation would encompass all components of the phytoplankton community (Arrigo, 2005). Here, both Ni and urea would be required for growth. More generally, low macronutrient concentrations in combination with low Ni could impose a scenario where only Ni–SOD using organisms are in a state of biochemically independent Ni–N or Ni–P colimitation. Here, the addition of N or P should result in growth of the entire community, whereas Ni additions should promote only select phytoplankton groups.

On the basis of extended micronutrient: macronutrient stoichiometry from the equatorial Pacific, Mackey et al. (2002) concluded that the $\sim 2.5 \text{ nmol L}^{-1}$ of the Ni in surface seawater from that region was biologically refractive, and that Ni limitation could occur in phytoplankton communities growing on urea if dissolved Ni concentrations approach this refractory limit. However, the potential for either Ni or Ni–urea colimitation in marine microbial assemblages has remained untested, perhaps because the concentrations of dissolved Ni in surface seawater are relatively high compared with those of Fe, Co, and Zn, metals shown to be limiting or colimiting to select marine phytoplankton communities (Crawford et al., 2003; Saito et al., 2005). However, Ni has slow ligand exchange kinetics relative to other metals, necessitating proportionately more membrane transporters and outer membrane space to attain an equivalent uptake rates (Hudson and Morel, 1993). Additionally, Ni may be bound by organic ligands, thereby reducing the bioavailable inorganic chemical species of the metal, possibly explaining the biologically refractory Ni suggested by Mackey et al. (2002). Ni speciation measurements in estuarine environments verified the presence of remarkably strong Ni-binding ligands (Bedsworth and Sedlak, 1999; Donat et al., 1994), though measurements in open ocean environments are sparse (Saito et al., 2004). To test the potential for Ni limitation or Ni–urea colimitation in a variety of surface ocean ecosystems, bottle-based fertilization experiments were used. In parallel, community-scale Ni uptake kinetics were determined to gain insight to the potential interactions between community composition, nitrogen biogeochemistry, and Ni cycling.

2. Methods

2.1. Station locations and sampling

The work presented here was conducted on three separate cruises, and the dates and locations of the sampling are detailed in Table 1 and Fig. 1. Water columns were characterized less than an hour prior to trace-metal clean sampling using a SeaBird CTD equipped with chlorophyll *a* (Chl *a*) fluorescence (Turner Instruments) and oxygen (Seabird) sensors. For all incubation experiments, surface seawater was pumped using an acid-washed Teflon-lined diaphragm pump and Teflon tubing directly from a depth of 3 m into an acid-washed low-density polyethylene (LDPE) carboy within a laminar flow bench. The inlet of the tubing was deployed 5 m away from the side of the vessel using a fiberglass pole while moving ahead slowly at 0.5–1 knot. Non-surface water samples were collected using Teflon-lined GO-FLO bottles deployed on poly line (LTER cruise) or mounted on a trace-metal clean rosette deployed on Kevlar line (Peru cruise). GO-FLO bottles were pressurized using ultra high purity nitrogen

Table 1
Locations and dates of experimental work.

Station name	General area	Date(s)	Latitude	Longitude	Type of experiment
GOCAL3	Gulf of California	6 August 2005	27.0°N	111.45°W	Uptake (kinetics), growout
PERU9	Peru-nearshore	20 October 2005	15.63°S	75.13°W	Uptake (tracer)
PERU12	Peru-offshore	22 October 2005	16.28°S	75.61°W	Uptake (tracer), Growout
PERU26	Peru-offshore	26 October 2005	12.0°S	78.65°W	Uptake (tracer)
LTER1	California Current	11 May 2006	34.30°N	120.8°W	Growout
LTER1	California Current	12 May 2006	34.35°N	120.9°W	Uptake (kinetics)
LTER2	California-offshore	16 May 2006	33.70°N	122.20°W	Growout
LTER2	California-offshore	12 May 2006	33.45°N	122.10°W	Uptake (kinetics)
LTER3	California-nearshore	23 May 2006	34.63°N	120.76°W	Uptake (kinetics)
LTER4	California Current	28 May 2006	34.03°N	121.56°W	Uptake (kinetics)
LTER5	California-offshore	1 June 2006	32.7°N	124.16°W	Growout
LTER5	California-offshore	2 June 2006	32.48°N	124.28°W	Uptake (kinetics)

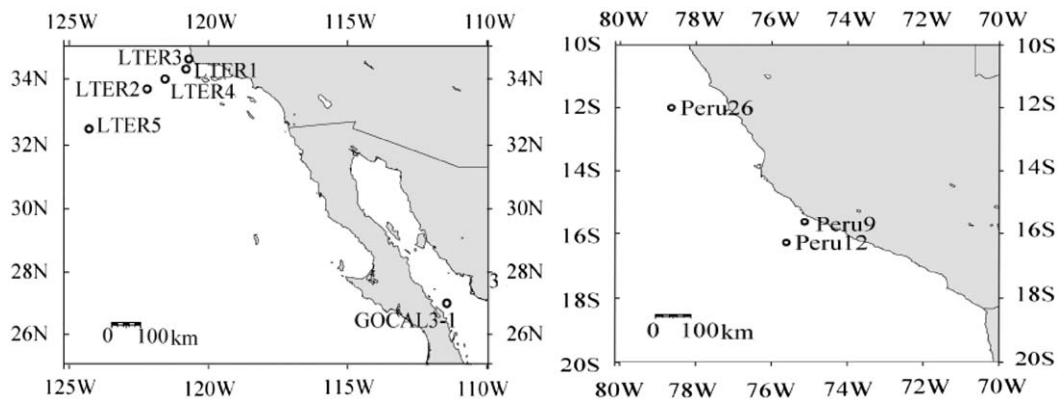


Fig. 1. Locations and station designations of work detailed in Table 1.

gas to force water directly into a laminar flow bench where subsampling occurred.

2.2. Fertilization experiments

Unfiltered surface seawater was dispensed to 12 2.7L polycarbonate bottles, which were treated in triplicate as follows: (1) No addition (controls), (2) 0.75 nmol L^{-1} Ni (a $4.05 \mu\text{L}$ addition from a stock of $500 \mu\text{mol L}^{-1}$ NiCl_2 in 0.037 M Ultrex grade HCl), (3) $2.5 \mu\text{mol L}^{-1}$ urea (filter-sterilized 1 mol L^{-1} stock made in Milli-Q), and (4) both Ni and urea additions as described above. Prior to filter sterilization, the urea stock was equilibrated with specially prepared chelex resin (Price et al., 1988/1989) and NH_4^+ contamination was always less than 1%, as determined using the indophenol method (Koroleff, 1983). Bottles were sealed and placed in on-deck seawater-flow-through incubators screened to 40% ambient light. All sampling and manipulations of the bottles were conducted in a laminar flow bench using trace-metal clean methods. Bottles were rigorously cleaned prior to the experiment using sequential washes of 1% soap (Citranox, 2 days), 10% HCl (Fisher trace metal grade, 2 days), and 1% HCl (2 days), with multiple rinses with Milli-Q water ($18.2 \text{ m}\Omega$, Millipore) following each step. Incubations were conducted as long as the temperature of the on-deck incubators could be maintained at $\pm 2^\circ\text{C}$ of the starting temperature.

2.3. Nutrient concentrations

Unfiltered seawater samples (40 mL) were dispensed into acid-washed 50 mL polyethylene tubes and frozen at -20°C until analyses (less than 3 months). Concentrations of nitrate, nitrite,

phosphorus, and silicate were determined at the Marine Analytical Facility of the University of California, Santa Barbara. Urea concentrations of unfiltered seawater were measured at the time of sampling using the diacetyl monoxime method (Revilla et al., 2005).

2.4. Dissolved nickel and iron concentrations

Seawater was filtered through acid-washed polycarbonate track-etched filters ($0.4 \mu\text{m}$ pore size, Millipore) in Teflon filter holders and catch vessels (Savillex). Filtered water was dispensed to acid-washed LDPE bottles and acidified ($\text{pH} \sim 1.8$, Ultrex HCl). Bottles were double-bagged and stored in the dark for at least 1 year. Competitive ligand exchange adsorptive cathodic stripping voltammetry (CLE-ACSV) was used to measure total dissolved Ni using the methods described in Saito et al. (2004). Briefly, 10 mL aliquots of seawater were neutralized to $\text{pH} = 8.0$ using ammonia (1 mol L^{-1} , quartz distilled) and buffered with $200 \mu\text{mol L}^{-1}$ $\text{pH} 8.0$ EPPS (4-(2-hydroxyethyl)-piperazinepropane-sulfonic acid; Sigma). The Ni chelator dimethyl glyoxime (DMG, Aldrich) was added to a final concentration of $100 \mu\text{mol L}^{-1}$ from a stock of 500 mmol L^{-1} . To reduce Ni contamination in the reagents, DMG was recrystallized in $100 \mu\text{mol L}^{-1}$ ethylenediamine tetraacetic acid (EDTA) and dissolved in Ultrex grade methanol and the EPPS was equilibrated with specially prepared Chelex-100 resin (Price et al., 1988/1989) prior to filter sterilization. Samples were analyzed on a BASi hanging mercury drop electrode and Epsilon E2 potentiostat (Bioanalytical Systems) run in linear sweep mode. Following a 2 min purge with ultra high purity nitrogen gas and a 90 s deposition at -0.7 V , a high speed scan from -0.7 to -1.4 V was conducted at a speed of 10 V s^{-1} . Nanomolar standard

additions of Ni (Fisher AAS stock diluted to 340 nmol L^{-1} in 0.1% v/v Ultrex grade HCl) were made to determine the original Ni concentrations. The method was validated using the surface sampling and analysis of Fe (SAFe) (Johnson et al., 2007) and NASS5 standards; SAFe reference value: $2.40 \pm 0.03 \text{ nmol L}^{-1}$ (M. Gordon, personal communication), measured value $2.43 \pm 0.05 \text{ nmol L}^{-1}$ and NASS5 reference value: $4.31 \pm 0.48 \text{ nmol L}^{-1}$, measured value $4.34 \pm 0.24 \text{ nmol L}^{-1}$. The standard error associated with this method on this instrument is significantly improved over previously published measurements made using different instruments (Donat and Bruland, 1988; Saito et al., 2004).

Acidified samples for total dissolved iron (Fe) were neutralized prior to analysis with 0.1 mol L^{-1} quartz-distilled ammonium hydroxide (Q-NH₄OH). Total dissolved Fe concentrations were then measured using adsorptive cathodic stripping voltammetry (ACSV) with the added ligand salicylaldoxime and borate buffer on the same instrument used for the Ni measurements (Buck et al., 2007). Detection limits for this method are on the order of 0.01 nmol L^{-1} , and this method successfully participated in the SAFe intercalibration cruise (Johnson et al., 2007); SAFe reference value: $0.097 \pm 0.043 \text{ nmol L}^{-1}$ (Johnson et al., 2007), measured value $0.100 \pm 0.015 \text{ nmol L}^{-1}$.

2.5. Chlorophyll concentrations

Seawater was filtered onto $0.2 \mu\text{m}$ pore size filters (polyethersulfone, Supor) that were placed in 10 mL of 90% acetone and incubated in the dark at -20°C for 12–24 h. Chlorophyll concentrations of room temperature samples were determined using a fluorometer calibrated using commercial chlorophyll standards (Turner Instruments, 10-AU).

2.6. Phytoplankton pigment analyses

One liter of seawater was gently filtered onto a Whatman GF/F filter, which was placed in a cryogenic vial and stored in liquid nitrogen until analysis as described in Goericke and Montoya (1998). For extraction of pigments, the filters were placed in 3 mL acetone, homogenized on ice with mortar and pestle, and allowed to incubate for 2 h (4°C , in the dark) following the addition of an internal standard (canthaxanthin in $50 \mu\text{L}$ of acetone). Prior to reverse-phase high performance liquid chromatography (HPLC) analysis, the filter extracts were centrifuged to remove cellular and filter debris. Samples ($200 \mu\text{L}$) of extract were manually injected onto a Waters HPLC system equipped with an Alltech Microsorp C-18 column and a UV-vis detector ($\lambda=440 \text{ nm}$). A ternary solvent system was employed for pigment separation and HPLC-grade solvents (Fisher) were used to prepare eluents A, B, and C: eluent A (MeOH:0.5 mol L⁻¹ ammonium acetate, 80:20), eluent B (methanol), and eluent C (acetone). The linear gradient used for pigment separation was (time in minutes' (%eluent A, %eluent B, and %eluent C)): 0.0' (0, 100, 0), 5' (0, 85, 15), 10.0' (0, 70, 30), 14' (0, 20, 80), 16.0' (0, 20, 80), and 18.0' (100, 0, 0). The eluent flow rate was held constant at 1 mL min^{-1} . Eluting peaks were identified by comparing their retention times with those of pigment standards and algal extracts of known pigment composition. Pigments were quantified using external standard curves and the UV-vis detector was calibrated spectrophotometrically using HPLC-purified pigment standards. To convert pigment concentrations to taxon level contributions to total Chl *a*, the ratios of the carotenoid pigments were optimized as described in Goericke and Montoya (1998).

2.7. Flow cytometry counts of picoplankton abundance

One-milliliter samples of seawater were dispensed to sterile 1.5 mL cryogenic vials and allowed to fix for 10 min with glutaraldehyde added to a final concentration of 0.25% v/v from a stock of 25% (Sigma Chemicals) prior to immediate storage in liquid nitrogen. The samples were analyzed on a Becton Dickson FACSsort flow cytometer using techniques described previously (Collier and Palenik, 2003). Green fluorescent beads ($0.9 \mu\text{m}$ -diameter, Duke Scientific) were added to a final concentration of 25–30 beads μL^{-1} as an internal standard. The instrument settings were optimized to examine the abundance and fluorescence characteristics of *Synechococcus*-like and Chl *a* containing piceoeukaryotic-like cells; the abundances of *Prochlorococcus*-like cells could not be confidently determined in some experiments and are not presented.

2.8. Ni uptake kinetics and rate measurements

In LTER uptake kinetics experiments, seawater was dispensed to twenty-four acid-washed bottles (polycarbonate, 60 mL, Nalge Nunc), eight bottles were also spiked with glutaraldehyde to a final concentration of 0.25% to serve as kill controls. Following 1 h, ⁶³Ni (Perkin Elmer, 9.87 mCi mg^{-1} Ni, stored in 0.037 M HCl, Ultrex grade) was added to the eight sets of one “kill” and two “live” bottles to achieve a range of eight added ⁶³Ni concentrations from 0.1 to 30 nmol L^{-1} . Following 4–6 h, samples were filtered onto $0.2 \mu\text{m}$ pore size filters (polyethersulfone, Supor). The GOCAL3 uptake kinetics experiment was identical except that 500 mL polycarbonate bottles were used and samples were split, with 100 mL being filtered through a $0.2 \mu\text{m}$ filter and the remainder being passed through a $5.0 \mu\text{m}$ filter.

In the Ni uptake experiments conducted in the Peru upwelling, only a limited amount of ⁶³Ni was available, therefore kinetics experiments were not possible. To attain a sense of the rate of ⁶³Ni uptake at these sites, 1 nmol L^{-1} additions of ⁶³Ni were added to triplicate 70 mL bottles, one of which was pretreated with 0.25% v/v glutaraldehyde as a kill control. Following 4–6 h, the bottle contents were passed through $0.2 \mu\text{m}$ pore size filters (Supor).

For all experiments, samples were incubated in the radiation laboratory at constant temperature under artificial grow lights. The incubation temperature was 18°C for the GOCAL and LTER experiments and 15°C for the Peru experiments. Neutral density screening was employed to mimic the light levels from the depth of sampling, based on profiles of photosynthetically active radiation (PAR) collected on CTD casts contiguous with incubation sampling.

Following collection of radiolabeled particulate material, filters were sequentially rinsed with 10 mL of 10 mmol L^{-1} sulfoxime (a Ni chelator dissolved in $0.2 \mu\text{m}$ -filtered seawater, Avocado Biochemicals) and 10 mL of $0.2 \mu\text{m}$ -filtered seawater to remove surface bound Ni and subsequently placed in 10 mL of scintillation cocktail (Ecolyte). Our experiments with diatom and cyanobacterial isolates have shown that sulfoxime rinses do not cause cell lysis (Dupont, unpublished). Radioactivity was assayed via scintillation counting on a Beckman LS1801 liquid scintillation counter. Seawater and phytoplankton biomass were found to have insignificant quench effects on ⁶³Ni activity. Samples were counted for ten minutes and counting errors were typically < 5%. DPM was converted to ⁶³Ni molarity using the specific activity of the stocks (Perkin Elmer, 9.87 mCi mg^{-1}). Linearity of the DPM-⁶³Ni relationship for each stock solution was confirmed via a dilution curve. Concentrations were corrected for sample volume changes to calculate molar particulate ⁶³Ni per liter, and

divided by the incubation time to obtain particulate Ni uptake rates for each bottle. ^{63}Ni uptake rates are presented as (mean (live samples) – kill treatment) \pm range (live treatments). As isotope equilibration was found not to occur (see Sections 3 and 4.5), the presented uptake rates are not extrapolated using the measured natural Ni concentrations.

2.9. Statistics and curve modeling

Where appropriate, the hyperbolic Michaelis–Menten equation was fitted to the ^{63}Ni uptake curves using a least squares non-linear regression in Matlab (Mathworks Software). Statistical analyses were performed with JMP 5.1 statistical software (SAS Institute). The effect of each treatment was assessed using a one-way analysis of variance (ANOVA) with post-hoc Tukey–Kramer tests.

3. Theory on the interpretation of uptake results

To convert the uptake of a stable or radioactive isotope to *in situ* uptake an underlying assumption of isotope equilibration is required. When the label isotope I' is added to a solution containing the natural isotope I , it is assumed that the resulting concentration available for uptake to the particulate phase is $I+I'$ (isotope equilibration). The observed uptake rate (ρ') of I' is then assumed to be proportional to the *in situ* uptake rate $\rho+\rho'$ according to the equation $\rho+\rho'=\rho'((I+I)/I')$. This seems appropriate for macronutrients, yet complexation of trace metals by organic ligands is pervasive in surface seawater (Morel et al., 2003). Feasibly, organic complexation could render the natural isotopes unavailable for equilibration with an added tracer isotope, particularly if the metal and ligand possess slow ligand exchange kinetics. If equilibration does not occur or is incomplete, the observed uptake is only that of the added isotope and the extrapolation to an *in situ* uptake rate would be flawed. To date, all studies of trace metal uptake in marine systems have assumed that equilibration occurs between the added isotope and the naturally present pool.

Whether isotope equilibration occurs cannot be determined with single addition experiments. However, if hyperbolic uptake kinetics (e.g. Michaelis–Menten) are obeyed, the measurement of radiotracer uptake rates ρ' for a range of I' with subsequent conversion to $\rho+\rho'$ should reveal the presence or absence of isotope equilibration. For illustrative purposes, the theoretical $\rho+\rho'$ uptake rates for a range of $(I+I')$ was calculated for an organism with traditional Michaelis–Menten kinetics ($V_{\max}=12$ and $K_{\rho}=3$) (Fig. 2A). What should be observed for ρ' in this scenario is also shown. Essentially, if complete isotopic equilibration does occur, a hyperbolic curve of $\rho+\rho'$ should be observed. Alternatively, if isotopic equilibration does not occur at all, the perceived uptake ρ' will only reflect I' (Fig. 2B). Then, through the application of the assumption that equilibration does occur, the calculated $\rho+\rho'$ will be invariant with regards to $I+I'$ (Fig. 2B). An intermediate scenario is that some equilibration occurs, but the amount available for uptake does not scale directly with $I+I'$.

The primary goal was to determine the Ni uptake kinetics of natural communities, therefore uptake rates were measured for a range of ^{63}Ni additions chosen to bracket the K_{ρ} displayed by marine *Synechococcus* (Dupont et al., 2008a). However, we did not assume *a priori* that the added ^{63}Ni isotope equilibrates with the stable non-radioactive Ni present in seawater, instead choosing to actually examine the extent of equilibration. If isotope equilibration does occur, the calculated $\rho+\rho'$ should resemble Fig. 2A and the ^{63}Ni uptake rates from the lowest level additions

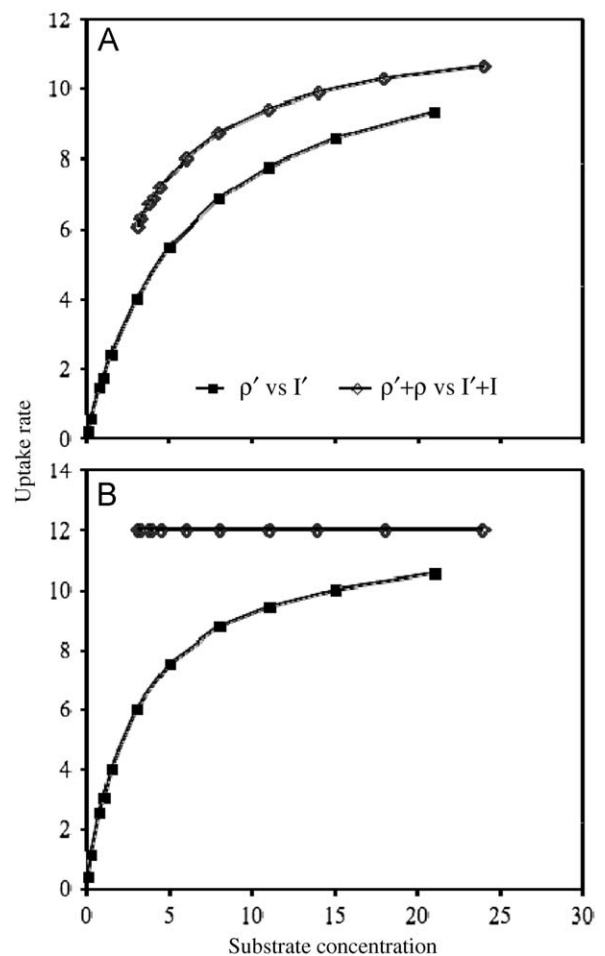


Fig. 2. Effects of isotope equilibration on the uptake of a tracer isotope. Plotted are the theoretical uptake by an organism with Michaelis–Menten kinetics ($V_{\max}=12$ and $K_{\rho}=3$). Panel A shows the uptake rates for just the radioisotope and both the radioisotope and stable isotope assuming complete isotope equilibration. Panel B displays the calculated shows the uptake rates for the radioisotope and both the radioisotope and stable isotope assuming no isotope equilibration.

(0.1 nmol L^{-1} , less than 3% of the natural Ni pool) can be extrapolated *in situ* uptake rates.

4. Results and discussion

4.1. Experimental overview

Table 1 and Fig. 1 provide the dates, locations, and a summary of the work conducted.

The response of phytoplankton communities to the additions of 0.75 nmol L^{-1} Ni (+Ni), $2.5\text{ }\mu\text{mol L}^{-1}$ urea (+urea), or both (Ni+urea) was examined in order to test the hypothesis that Ni limitation or Ni–urea colimitation can occur in natural waters. Bottle-based fertilization experiments were conducted at GOCAL3, Peru12, LTER1, LTER2, and LTER5 (Fig. 1, Table 1) and the incubation length, initial macronutrient, Fe, and Ni concentrations are shown in Table 2. Two experiments (PERU12 and LTER1) began with relatively high particulate Chl *a* concentrations typical of recently upwelled macronutrient-replete waters but exhibited a 10-fold difference in Fe concentrations (Table 2). The other 3 experiments were conducted with low Chl *a* nitrogen-deplete phosphate-replete surface waters overlying stratified water columns (Table 2). The urea additions substantially

Table 2
Summary of Ni and urea fertilization experiments.

	Incubation					
	Treatment	GOCAL3	Peru12	LTER1	LTER2	LTER5
Length (h)		48	102	77	75	95
Ni (nmol L ⁻¹)	<i>t</i> =0	3.1 ± 0.07	4.19 ± 0.04	4.6 ± 0.5	3.47 ± 0.05	3.84 ± 0.18
Fe (nmol L ⁻¹)	<i>t</i> =0	3.67 ± 0.05	0.17 ± 0.03	1.96 ± 0.04	0.37 ± 0.02	0.13 ± 0.03
Chl <i>a</i> μg L ⁻¹	<i>t</i> =0	0.15	1.19	2.6	0.045	0.087
	Control	0.14 ± 0.01 A	1.35 ± 0.18 A	16.6 ± 1.8 A	0.049 ± 0.01 A	0.078 ± 0.01 A
	Ni	0.22 ± 0.03 a	1.50 ± 0.07 A	19.2 ± 1.0 A	0.065 ± 0.01 A	0.076 ± 0.02 A
	Urea	0.96 ± 0.01 B	1.50 ± 0.17 A	23.4 ± 2.0 A	0.32 ± 0.09 B	0.42 ± 0.06 B
	Ni+urea	0.99 ± 0.1 B	2.59 ± 0.00 B	20.9 ± 2.4 A	0.34 ± 0.07 B	0.38 ± 0.02 B
Urea μmol L ⁻¹	<i>t</i> =0	< 0.1	< 0.1	0.22 ± 0.01	< 0.1	< 0.1
	Control	< 0.1	< 0.1	< 0.1	< 0.1	< 0.1
	Ni	< 0.1	< 0.1	< 0.1	< 0.1	< 0.1
	Urea	< 0.1	1 ± 0.3	< 0.1	2 ± 0.2	< 0.1
	Ni+urea	< 0.1	< 0.1	< 0.1	1.9 ± 0.2	< 0.1
NO ₃ +NO ₂ μmol L ⁻¹	<i>t</i> =0	< 0.1	10.75	8.6	< 0.1	< 0.1
	Control	< 0.1	7.06 ± 0.36 A	0.11 ± 0.02	< 0.1	< 0.1
	Ni	< 0.1	6.13 ± 0.8 A	< 0.1	< 0.1	< 0.1
	Urea	< 0.1	7.8 ± 0.25 A	< 0.1	< 0.1	< 0.1
	Ni+urea	< 0.1	6.8 ± 0.1 A	< 0.1	< 0.1	< 0.1
PO ₄ μmol L ⁻¹	<i>t</i> =0	0.4	1.56	0.7	0.25	0.16
	Control	0.34 ± 0.03 A	1.28 ± 0.02 A	0.13 ± 0.01 A	0.24 ± 0.1 A	0.15 ± 0 A
	Ni	0.33 ± 0 A	1.25 ± 0.02 A	0.14 ± 0.01 A	0.17 ± 0.01 A	0.16 ± 0.01 A
	Urea	0.29 ± 0.01 A	1.33 ± 0.08 A	0.15 ± 0 A	0.15 ± 0.02 A	0.13 ± 0 A
	Ni+urea	0.25 ± 0 B	1.15 ± 0.02 B	0.15 ± 0 A	0.15 ± 0.02 A	0.15 ± 0 A
SiO ₃ μmol L ⁻¹	<i>t</i> =0	2.7	7.9	2.7	2.16	1.7
	Control	2.4 ± 0 A	3.4 ± 0.35 A	1.3 ± 0.1 A	1.5 ± 0.26 A	1.3 ± 0.15 A
	Ni	2.35 ± 0.05 A	2.63 ± 1.1 A	1.5 ± 0.2 A	1.6 ± 0.5 A	1.5 ± 0.2 A
	Urea	2.25 ± 0.05 A	3.15 ± 0.5 A	1.4 ± 0.1 A	1.3 ± 0.15 A	0.9 ± 0.5 A
	Ni+urea	2.4 ± 0.1 A	2.3 ± 0.5 A	1.4 ± 0.2 A	1.4 ± 0.45 A	1.7 ± 0.1 A
<i>Synechococcus</i> 10 ³ cells mL ⁻¹	<i>t</i> =0	64	38	2.3	38	15.3
	Control	74 ± 18 A	25 ± 0 A	43.4 ± 4.9 A	20.6 ± 1.1 A	6.0 ± 0.6 A
	Ni	219 ± 61 B	31 ± 12.1 A	45.6 ± 2.1 A	15.7 ± 4.0 A	6.7 ± 2.5 A
	Urea	1416 ± 209 C	15.6 ± 6.3 A	47.1 ± 4.5 A	44.8 ± 2.2 B	28.4 ± 1.5 B
	Ni+urea	1727 ± 59 C	31 ± 18 A	52.4 ± 5.5 A	46.3 ± 3.1 B	29.7 ± 1.9 B
<i>Picoeukaryotes</i> 10 ³ cells ml ⁻¹	<i>t</i> =0	2.1	102	2.9	13.5	6.8
	Control	6.4 ± 0 A	46 ± 9.9 A	164.8 ± 10.2 A	12.2 ± 0.7 A	8.9 ± 1.3 A
	Ni	8.4 ± 0 a	51.6 ± 10.4 A	161.1 ± 12.4 A	13.4 ± 1.8 A	10.8 ± 2.8 A
	Urea	17.5 ± 4.0 B	41.5 ± 8.3 A	207 ± 18.3 B	44.7 ± 4.4 B	38.6 ± 3.6 B
	Ni+urea	20.6 ± 2.0 B	50.3 ± 8.7 A	200 ± 36.6 B	41.1 ± 4.5 B	35.8 ± 4.4 B

Standard deviations are for 3 replicate bottles. The different experiments were analyzed with a one-way ANOVA with post-hoc Tukey–Kramer tests to determine significant ($p < 0.05$) differences between the treatment means. Values marked with a different letters (e.g. A or B) have different means. The two cases where a slightly relaxed cutoff ($p < 0.1$) results in a significant difference are noted by a lower case letter.

increased the total nitrogen at the beginning of each experiment except for Peru 12 and LTER1, where the increase was ~50%. The Ni additions increased concentrations by less than 25%. All of the incubations were conducted with water collected from 3 m. In the case of the LTER2, LTER 5, Peru12, and GOCAL3 experiments, the water was collected from a shallow mixed layer and the incubation at 40% PAR is likely close to the daily average. The water column at LTER1 was well mixed to 50 m; therefore the incubation at 40% PAR represents a high light treatment. In each of these cases, the no addition treatment provides a control for light effects. The incubations were conducted for as long as the seawater flow-through on-deck incubators could be maintained at a temperature similar to that of the original sampling site; therefore each experiment was conducted for different lengths of time (Table 2). While this precludes any absolute comparison between the magnitudes of observed changes, the focus is on the relative trends within the addition matrix.

Uptake experiments were conducted at every site, though due to a reduced availability of radiotracer, kinetics based uptake experiments were not conducted in Peru. Pilot experiments on a

cruise to the Gulf of California in 2004 were used to examine the temporal aspects of Ni uptake in untreated and glutaraldehyde-fixed samples. Following a 10 nmol L⁻¹ addition of ⁶³Ni to a natural surface phytoplankton community, ⁶³Ni uptake by the particulate phase in the kill control and live sample was equal and rapid for 1–2 min, followed by a plateau in the kill control and a gradual increase in particulate ⁶³Ni in the live sample. The end-time-point kill control therefore accounts for both the rapid equilibration generally measured with a *t*₀ control and the slower abiotic adsorption to bottles walls or particles over the entire experiment. Uptake in the live control proceeded linearly for 6–8 h, after which the rates declined. For a 1 nmol L⁻¹ ⁶³Ni addition, uptake rates in the live samples proceeded linearly for 24–36 h (data are not shown). The linearity of uptake during these time periods indicates that the added Ni or the incubation conditions did not influence uptake rates. Based upon these results, all subsequent uptake experiments were conducted for less than 6 h and included a 0.25% glutaraldehyde end-time-point kill control which was ~10% of the experimental treatment. All data are presented as live-kill control.

4.2. Gulf of California experiments

Samples from the Gulf of California (GOCAL3) were collected in the summer of 2005 from the nitrate-deplete surface of a strongly stratified water column in the Guaymas Basin (White et al., 2007). The Gulf of California appears to be enriched in Fe and Mn relative to the Pacific (Huerta-Diaz et al., 2007), possibly due to the dust and rain deposition from the summer thunderstorms sweeping off the Sonoran desert noted in sediment trap records (Baumgartner et al., 1991; Thunell, 1998). The seemingly high Fe concentrations presented for the GOCAL3 experiment (Table 2) are consistent with this. In the GOCAL3 fertilization experiment, the +urea and Ni+urea treatments prompted similar increases in Chl *a* and picoplankton, suggesting a level of nitrogen limitation (Table 2). Ni additions resulted in a modest increase in Chl *a* concentrations ($p < 0.1$, ANOVA), a 3-fold increase in *Synechococcus* abundances ($p < 0.05$, ANOVA), and a 30% increase in picoeukaryote abundance ($p < 0.1$, ANOVA, Table 2). The responses to the +Ni treatment were less in magnitude relative to the +urea and Ni+urea treatments. High zeaxanthin (zeax) concentrations indicate that the phytoplankton community was dominated by *Synechococcus*-like cyanobacteria, with divinyl Chl *a* concentrations being below detection at the beginning of the experiment (Fig. 3A). 19'Hexanoyloxy fucoxanthin (19'hex)-containing prymnesiophytes may have also contributed to the total Chl *a* (community composition calculations not shown). After the 48 h incubation following nutrient additions, the +urea and Ni+urea treatments were virtually indistinguishable from each other, but were significantly enriched compared with control bottles for all detected pigments (Fig. 3A, $p < 0.05$, ANOVA). The +Ni treatment had significant increases only for total Chl *a*, the *Synechococcus* pigment zeax, and the *Prochlorococcus* pigment divinyl Chl *a* relative to the control bottles ($p < 0.05$, ANOVA, Fig. 3A). Essentially, the combined pigment and flow cytometry data show that the entire phytoplankton community responded to urea additions but that only the cyanobacteria and picoeukaryotes were influenced by Ni.

The cyanobacteria (and to a lesser extent, *Ostreococcus*-like picoeukaryotes) of Gulf of California community appears to be Ni-urea colimited in a biochemically independent fashion (Saito et al., 2008), with both Ni and urea additions inducing some

growth. While both cyanobacteria and picoeukaryotes require Ni to assimilate urea, there were no significant differences between the Ni+urea and +urea treatments. The cyanobacteria do appear to have been primarily nitrogen limited, as the urea additions prompted a greater increase in cell abundance, zeax, and divinyl chl *a* relative to Ni additions. The urea and Ni+urea treatments also resulted in increased phycoerythrin fluorescence per *Synechococcus* cell (data are not shown), which likely reflects the rapid synthesis of the N-rich phycobiliproteins that occurs in *Synechococcus* following the relief of nitrogen limitation (Wyman and Gregory, 1985). This effect was not observed for Ni additions, thus it seems unlikely that the observed responses in the +Ni treatment are due to an increased ability to assimilate urea. The subnanomolar Ni addition is unlikely to have inhibited grazers of cyanobacteria and picoeukaryotes as these organisms have Ni toxicity thresholds in the micromolar range (Kszos et al., 1992), and a similar effect was not observed in the other experiments. Alternatively, the cyanobacteria and picoeukaryotes may have been Ni limited due to the usage of Ni-SOD. In this scenario, the addition of Ni restores Ni-SOD activity, improving oxidative defense and facilitating growth for a brief period, though nitrogen limitation will cap overall growth. In these organisms, urease and Ni-SOD must split the intracellular Ni pool. Therefore, the urea-induced relief from nitrogen limitation may have reduced oxidative stress and, consequently, the biological need for Ni-SOD, which may account for the apparent lack of synergistic effects in the Ni+urea treatments.

^{63}Ni uptake rates were determined for a range of ^{63}Ni additions in two size fractions (0.2–5.0 μm and $> 5.0 \mu\text{m}$) of a microbial community from the surface (Fig. 4). The ^{63}Ni uptake rates in the 0.2–5.0 μm and $> 5.0 \mu\text{m}$ size fractions were well modeled by Michaelis–Menten kinetics (fitted curves in Fig. 4A), with a K_p of 3 nmol L^{-1} for both size fractions (Table 3). At each ^{63}Ni addition, the 0.2–5.0 μm size fraction exhibited ^{63}Ni uptake rates nearly an order of magnitude greater than those observed for the $> 5.0 \mu\text{m}$ size fraction (Fig. 4A), highlighting the importance of this microbial size fraction to Ni biogeochemistry. The decline in $> 5.0 \mu\text{m}$ ^{63}Ni uptake rates for the highest ^{63}Ni addition is assumed to be the result of Ni toxicity or a negative feedback regulation of Ni uptake in this size fraction, as observed in similar studies with phytoplankton

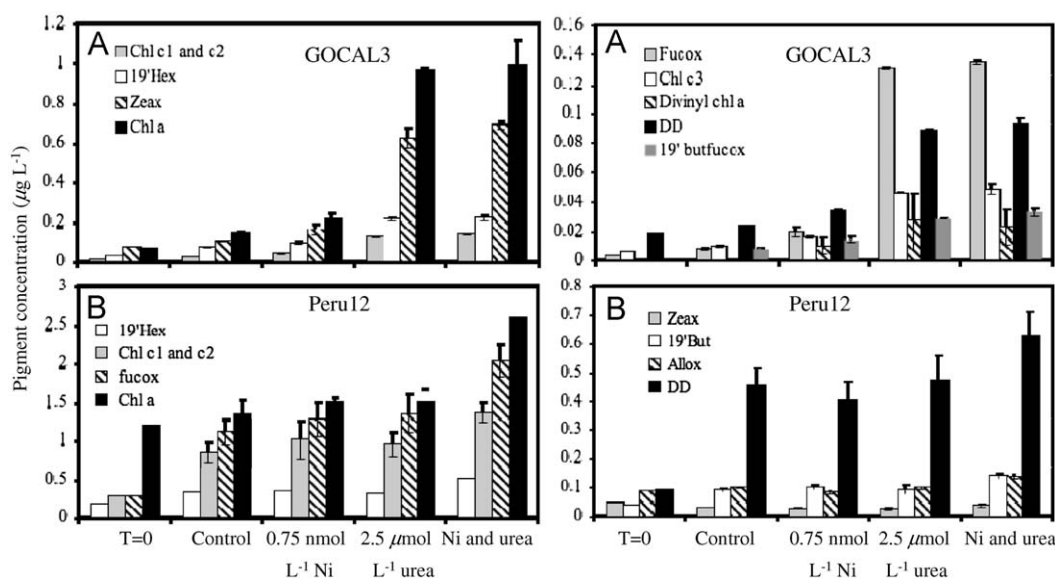


Fig. 3. Effects of Ni and urea on phytoplankton communities. Shown are the most abundant phytoplankton pigments in the beginning and end of the bottle incubation experiments conducted at (A) GOCAL3 and (B) Peru12. Error bars are the standard deviations of triplicate bottles.

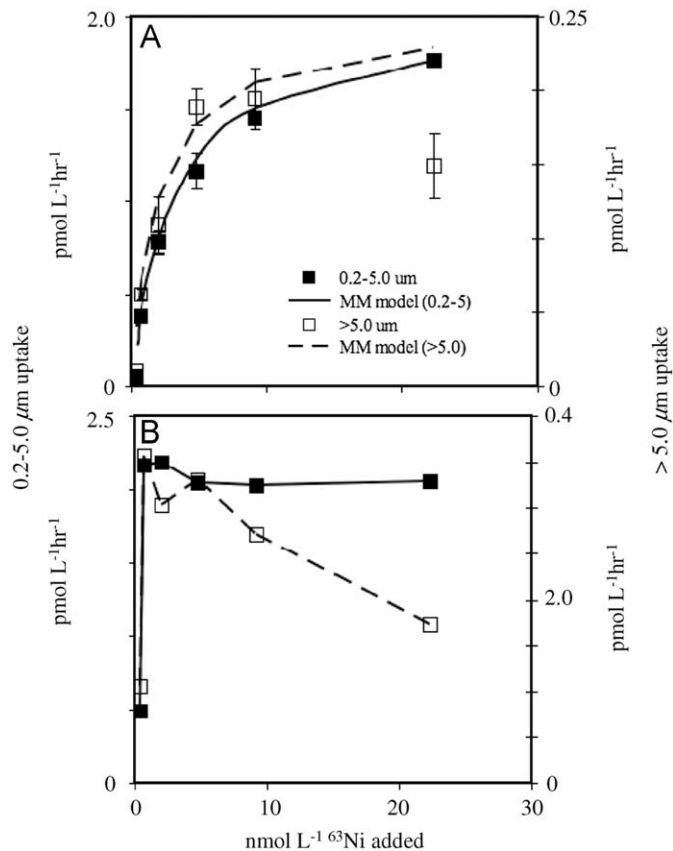


Fig. 4. ^{63}Ni uptake kinetics at GOCAL3: (A) Absolute ^{63}Ni uptake rates observed for the 0.2–5.0 μm and > 5.0 μm size fractions over a range of ^{63}Ni additions. Also shown are the fitted least squares regression models of the Michaelis–Menten equation. (B) calculated *in-situ* Ni uptake (both stable and radioactive Ni) for the same size fractions. Error bars are the range of duplicate kill control corrected bottles.

monocultures (Sunda and Huntsman, 1992). The calculated *in situ* Ni uptake rate did not follow the model behavior (Fig. 4B), indicating that the added radioisotope did not equilibrate with the stable Ni.

4.3. California current LTER experiments

The California Current Ecosystem Long Term Ecological Research (LTER) cruise was in May 2006 and complete hydrographic data for each site is available at <http://cce.lternet.edu/data/cruises/cce-p0605/data>. LTER1, a coastal site near Point Conception, was characterized by a recently-upwelled, nitrate-rich water column. Near the outer edge of the North Pacific subtropical gyre, LTER2 and LTER 5 were in stratified environments with negligible NO_3^- within a narrow (10 m) surface mixed layer and a relatively deep (70–75 m) subsurface Chl *a* maximum. LTER3 was in a shallow, stratified, and nutrient rich coastal area, and LTER4 was in a recently mixed, low nitrate “mesotrophic” water column with a subsurface Chl max at 50 m.

The LTER2 and LTER5 experiments both started with nitrogen deplete waters, and urea additions, with or without Ni, resulted in significant increases in particulate Chl *a* and the abundances of picoeukaryotes and *Synechococcus*-like cyanobacteria. Synergistic effects were not observed for the Ni+urea treatments, and the +Ni treatments did not prompt any noticeable biological effects relative to the controls (Table 2). Almost none of the additions resulted in statistically significant differences in the measured

parameters for the LTER1 experiment, which started with nutrient replete water from a deeply mixed water column. Here, the incubation at a constant light level of 40% PAR likely removed light limitation in a nitrate rich water sample, explaining the increases in biomass and nutrient drawdown seen for all treatments. The urea additions did prompt modest increases in the numbers of picoeukaryotes in this incubation (Table 2). Ni limitation was not observed in the LTER experiments, yet some *Synechococcus* strains (eg. WH7803 and WH7805) use an Fe–SOD instead of a Ni–SOD, presumably avoiding the obligate Ni requirements (Dupont et al., 2008b). The response of *Synechococcus* to urea additions in the LTER and GOCAL fertilizations (Table 2) is consistent with the emerging paradigm of urea being particularly important to the ecology of this organism (Heil et al., 2007).

^{63}Ni uptake kinetics were determined for communities collected from multiple depths in several different regimes of the California Current in the spring of 2006, but only for the > 0.2 μm size fraction. The results of the uptake experiments from three depths at the LTER3 station are shown in Fig. 5, while complete information for all experiments is in Table 3. At LTER 3, increasing depth and decreasing particulate Chl *a* results in increasing half saturation constants and decreasing maximal uptake rates (Table 3, Fig. 5A). As observed with the GOCAL kinetics experiments, the assumption that the added radioisotope equilibrates with the stable Ni results in an aberrant curve for *in-situ* Ni uptake (Fig. 5B). Similar curves were obtained at all other stations, indicating that the added ^{63}Ni did not properly equilibrate with the stable Ni.

4.4. Peru experiments

Stations Peru9, Peru12, and Peru26 were studied during October 2005, with the former two located in a high nitrate low chlorophyll (HNLC) regime where phytoplankton growth was shown to be limited by low levels of the micronutrient Fe in separate bottle incubation experiments (Moffett and John, personal communication). Iron limiting conditions at the fertilization station, Peru 9, are also supported by the high NO_3^- (μM)/Fe(nM) ratio at that station (~ 63). In contrast to the other four fertilization experiments, urea additions had little effect relative to the controls in the Peru12 experiment; only Ni+urea additions prompted a significant increase in Chl *a* levels over the controls ($p < 0.05$, ANOVA, Table 2). Dissolved PO_4^{3-} was also drawn down to a greater extent in the Ni+urea treatment compared with the other treatments (Table 2). Further, the added urea was completely removed in the Ni+urea treatment but not the +urea treatment where 40% of the original addition remained. The flow cytometry results indicate that the increased Chl *a* and nutrient drawdown was not due to increased picoplankton populations. HPLC-based pigment measurements revealed the $t=0$ community was rich in the diatom pigment fucoxanthin (fucox), and pigment ratios suggested that the community was almost entirely composed of diatoms (community composition calculations not shown), with only minor contributions by cryptophytes and pelagophytes. Substantial increases in the diatom pigment fucox were observed in the Ni+urea treatment relative to the other treatments ($p < 0.05$, ANOVA, Fig. 3B), suggesting the PO_4^{3-} drawdown is due to growth of diatoms. More modest increases in alloxanthin, 19’butanoyloxy fucoxanthin (19’but) and zeax concentration implies that the cryptophyte and pelagophyte portions of the community also responded to a lesser extent. While it is possible that the observed increases in phytoplankton pigments may be due to increased cellular pigment concentrations rather than increased cellular abundance, this would still

Table 3
Summary of all ⁶³Ni uptake experiments.

Station	Depth (m)	Chl <i>a</i> (µg L ⁻¹)	Ni uptake for 1 nM additions		Ni uptake kinetics		Dissolved Ni (nmol L ⁻¹)	NO ₃ (µmol L ⁻¹)	SiO ₃ (µmol L ⁻¹)	PO ₄ (µmol L ⁻¹)	Temperature (°C)	Oxygen (µmol L ⁻¹)
			(pmol L ⁻¹ h ⁻¹)	(pmol h ⁻¹ µg Chl <i>a</i> ⁻¹)	V _{max} (pmol L ⁻¹ h ⁻¹)	K _p (nmol L ⁻¹)						
GOCAL3	3	0.18	0.90	5.0	30	3	3.63+0.13	0	2	0.72	30.2	191
LTER1	3	4.74	13.30	2.8	129	34	4.6+0.5	8.6	11.8	0.71	11.3	211
LTER1	35	1.27	2.80	2.2	110	39	5.07+0.17	9.4	12.9	0.78	11.2	205
LTER2	5	0.01	1.74	174.0	28	11	3.45+0.09	0.06	2.16	0.2	14.3	252
LTER2	40	0.12	1.10	9.4	16	5	3.41+0.14	0.07	2.03	0.19	14	253
LTER2	75	0.49	11.70	23.9	132	26	3.51+0.12	1.75	3.85	0.36	14	251
LTER3	2	6.50	40.20	6.2	207	6	4.05+0.04	1.64	4.1	0.31	14.1	310
LTER3	12	3.75	6.10	1.6	39	8	4.3+0.14	5.37	11.81	0.58	13.4	300
LTER3	25	2.25	4.80	2.1	43	23	4.31+0.18	7.7	13.05	0.7	12	213
LTER4	10	1.11	9.70	8.7	6	1	3+0.05	0.95	3.43	0.25	14.7	248
LTER4	50	0.80	5.20	6.5	31	7	3+0.05	11.05	10.14	0.9	10.9	170
LTER5	5	0.12	2.60	21.5	25	10	3.84+0.18	0.105	1.67	0.23	16.2	240
LTER5	50	0.55	6.30	11.4	49	9	3.81+0.09	0.117	1.7	0.22	15.3	252
LTER5	78	0.56	5.50	9.9	103	15	4.14+0.1	4.63	5.3	0.56	12.6	232
Peru9	5	0.12	0.20	1.6	n/a	n/a	3.86+0.19	9.4	10.8	0.7	16.6	228
Peru9	20	0.36	0.40	1.1	n/a	n/a	4.37+0.21	10	7	0.7	16.3	225
Peru9	30	0.38	0.40	1.0	n/a	n/a	3.9+0.15	10.5	5.5	0.7	14.7	135
Peru9	40	0.19	0.13	0.7	n/a	n/a	4.12+0.18	12	18	1.2	14.3	40
Peru9	50	0.00	0.18	n/a	n/a	n/a	5.98+0.18	14.9	26.4	1.6	13.5	1.8
Peru9	70	0.00	0.36	n/a	n/a	n/a	5.44+0.18	14.8	33	1.6	13.2	1.8
Peru12	10	0.87	0.30	0.3	n/a	n/a	4.19+0.14	10.9	10.4	0.7	15.5	204
Peru12	20	1.13	0.30	0.3	n/a	n/a	4.66+0.22	10	10	1	15.3	192
Peru12	30	0.72	0.27	0.4	n/a	n/a	4.51+0.23	10	10	1	15.3	184
Peru12	45	0.81	0.31	0.4	n/a	n/a	5.3+0.19	10	10	1	13.8	43
Peru12	65	0.13	0.12	1.0	n/a	n/a	4.77+0.29	9.1	12.6	1.1	13.2	1.9
Peru12	100	0.08	0.13	1.7	n/a	n/a	4.55+0.15	15.6	32.2	1.5	12.7	1.8
Peru26	8	n/a	0.51	n/a	n/a	n/a	3.89+0.11	10.1	0.6	1.6	16.7	223
Peru26	70	n/a	0.44	n/a	n/a	n/a	4.55+0.15	20.8	1.5	12.4	14.1	3
Peru26	200	n/a	0.11	n/a	n/a	n/a	5.79+0.16	11.9	1.4	16.7	11.9	1.8
Peru26	300	n/a	b/d	n/a	n/a	n/a	6.39+0.13	31.5	2.1	35.8	10.7	2
Peru26	400	n/a	0.00	n/a	n/a	n/a	7.09+0.21	36.7	2.4	41.7	9.4	2
Peru26	500	n/a	b/d	n/a	n/a	n/a	7.15+0.23	41.1	2.7	49.6	8.1	6
Peru26	600	n/a	0.29	n/a	n/a	n/a	7.72+0.13	43.3	2.5	57.6	7	8
Peru26	1000	n/a	0.16	n/a	n/a	n/a	9.17+0.17	42.4	2.5	90.1	4.6	42

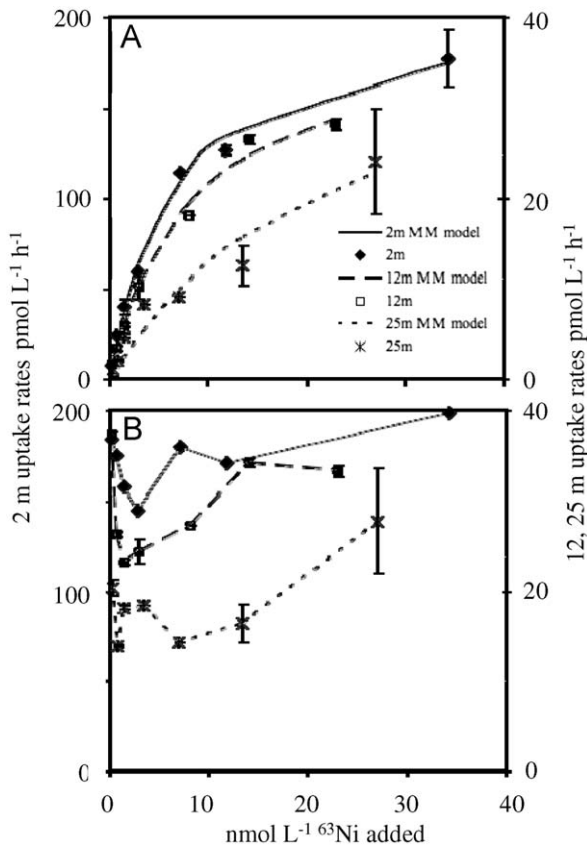


Fig. 5. ^{63}Ni uptake kinetics at LTER3: (A) Absolute ^{63}Ni uptake rates for a range of ^{63}Ni additions at water collected from 3, 12, and 25 m at LTER3. Also shown are the fitted Michaelis–Menten curves. Error bars are the range of duplicate kill control corrected bottles. (B) Calculated *in-situ* Ni uptake for the same depths and additions.

indicate a reprieve from some nutrient limitation. Both the picoeukaryotes and *Synechococcus* populations declined during the incubation experiments. While an exact reason is unknown, potentially the longer incubation period of this incubation (Table 2) introduced bottle effects detrimental to these smaller phytoplanktons. For example, grazers for cyanobacteria may be more abundant, and less likely to be diluted out by the subsampling inherent to bottle based incubations. This would result in a higher grazing rate for these smaller phytoplanktons over a longer period.

In terms of initial conditions, Peru12 and LTER1 both were N-, P-, and Si-replete, but vastly different in terms of Fe concentrations (Table 2). In Peru12, the low Fe concentrations may trigger a cascade of type III biochemically-dependent colimitations, where the assimilation of one substrate is dependent upon the presence of another substrate (Saito et al., 2008). Due to the role of Fe in NO_3^- and NO_2^- reduction, low ambient Fe can limit nitrate uptake resulting in Fe-nitrogen colimitation (Price et al., 1991). The addition of the reduced nitrogen source, urea, could relieve the nitrogen limitation provided Ni is bioavailable. Since increased nutrient drawdown and phytoplankton biomass were only observed in the Ni+urea additions, it follows that the +urea treatments became Ni-Fe-urea colimited (Table 2). Biochemically, the addition of Ni allows the hydrolysis of urea by the Ni metalloenzyme urease, providing a nitrogen source for growth and additionally relieving Fe requirements associated with the Fe-metalloenzymes nitrate and nitrite reductase.

Only a limited amount of ^{63}Ni was available for the field work in Peru; therefore depth profiles of kill-control corrected ^{63}Ni

uptake rates were compiled at Peru9, Peru12, and Peru26 using 1 nmol L⁻¹ additions of ^{63}Ni (Table 3). Peru9 and Peru12 were part of a cross-shelf transect in Southern Peru, a region where the upwelled waters are deficient in Fe relative to the other macronutrients, leading to Fe limitation in the surface waters (Bruland et al., 2005). Both sites were high in nitrate, with a subsurface Chl *a* maxima overlying a suboxic zone (Table 3). ^{63}Ni uptake rates were elevated in surface waters at both stations, with a decline in the oxycline. At station 9, uptake rates increased sharply below the oxycline to values similar to those observed in surface waters, despite no measurable Chl *a*. A profile offshore of the broad continental shelf (Peru26, Fig. 1) examined ^{63}Ni uptake rates and Ni concentrations over the upper kilometer of the water column (Table 3). ^{63}Ni uptake rates of hundreds of femtomoles L⁻¹ h⁻¹ were observed at several depths within the deep suboxic zone, suggesting that heterotrophic prokaryotes in the ocean's interior actively assimilate Ni, albeit at rates lower than those in the euphotic zone. Ni uptake outside of the euphotic zone may be linked to urea decomposition (Cho and Azam, 1995) and is consistent with the observation of genes for a Ni-containing urease and a Ni transporter in the genomes of both Bacterial and Archaeal NH_4^+ -oxidizers (Hallam et al., 2006; Klotz et al., 2007).

4.5. Trends in Ni uptake kinetics and rates across oceanic regions

Across the fifteen Ni uptake kinetics experiments, each including uptake rates for 8 different Ni concentrations, the added ^{63}Ni did not equilibrate with the natural pools of Ni. This renders the extrapolation of the observed ^{63}Ni uptake rates to an estimation of an *in situ* assimilation rate erroneous. The lack of isotope equilibration also precludes the extrapolation of metal and carbon uptake rates to estimated *in situ* metal:C ratios as has been done previously (Dixon et al., 2006; Schmidt and Hutchins, 1999; Strzepek et al., 2005). It is not known what prevents the equilibration of the added ^{63}Ni and the natural Ni, though complexation by organic ligands or the slow ligand exchange kinetics of Ni could be responsible. It is not known if this phenomenon is important for other metals, as most studies have extrapolated to *in situ* rates from single concentration additions. An examination of the assumption of isotope equilibration may require the measurement of the absolute uptake rates for a range of isotope additions. Certainly, Ni, with very slow ligand exchange kinetics, might be a special case.

Despite the lack of isotope equilibration in this study, we have used our measurements of ^{63}Ni uptake rates as a first approach to determine the affinity of the microbial community for inorganic Ni. There is in general a dearth of information on trace metal uptake kinetics in marine systems (with the exception of Maldonado et al., 2001), and our experiments, though not reflective of *in situ* uptake rates, significantly expand current knowledge in this area. Across all experiments, a correlation was observed between V_{max} and Chl *a* ($r^2=0.48$, $p < 0.05$, model II geometric mean linear regression). While other correlations were not observed across all samples, the depth dependent trends varied between oligotrophic and nutrient-rich sites. At LTER1 and LTER3, both V_{max} and K_p declined with Chl *a*. In the stratified oligotrophic sites LTER2 and LTER5, maximum V_{max} values were observed at the subsurface Chl *a* maximum, while the highest affinity for Ni was observed in the surface waters (Table 3). Only two depths were analyzed at LTER4, but they displayed similar trends in V_{max} and K_p to those observed at LTER3. Healey (1980) argued that the ratio $V_{\text{max}}:K_p$, also known as the specific affinity (Button, 1998), describes an organism's or community's competitive advantage in nutrient acquisition, with higher values of $V_{\text{max}}:K_p$ indicating an increased ability to acquire the nutrient at

low concentrations. When V_{\max} is normalized to Chl *a* to account for community biomass, the highest $V_{\max} \cdot K_p$ values were observed in the surface waters of the N-deplete GOCAL3, LTER2, and LTER5. These values should be treated with caution, as the normalization of V_{\max} with Chl *a* may be inappropriate given the natural variability of Chl *a* to carbon content and because non-photosynthetic microorganisms likely contribute to the observed Ni uptake. Another caveat involves organic complexation of Ni; if a portion of the added ^{63}Ni is complexed and rendered unavailable to uptake, this would artificially reduce uptake rates at the lowest additions and result in an overestimate of K_p . Nevertheless, the higher affinity for Ni at the nitrate-deplete sites and depths, which typically exhibit greater urea rates (Wafar et al., 1995), implies that microbial communities modulate Ni uptake according to nitrogen nutrition.

Dissolved Ni concentrations are clearly influenced by biological uptake; the macronutrients PO_4^{3-} , NO_3^- , and $\text{Si}(\text{OH})_4$ were correlated with Ni over the entire dataset ($r^2=0.81$, 0.81 , and 0.85 , respectively, model II geometric mean linear regression). To gain an appreciation for how Ni uptake varies between oceanic regions, the results of the Peru ^{63}Ni uptake rate measurements were compiled with the ^{63}Ni uptake rates for 1 nmol L^{-1} ^{63}Ni additions from the GOCAL and LTER kinetics experiments (Table 3). While the lack of isotopic equilibration precludes any determination of actual Ni uptake rates, the relative trends between experiments should be at least proportional to the *in-situ* uptake rates. The uptake rates for 1 nmol L^{-1} additions correlated with Chl *a* concentrations ($r^2=0.68$, model II geometric mean linear regression), but not with the concentrations of Ni or macronutrients. When compared with Chl *a* concentrations, Ni uptake rates were over an order of magnitude lower at the Peru upwelling sites compared with sites in the Gulf of California and California waters (Fig. 6). It seems unlikely that the difference was methodological, though the radiation laboratory used on the Peru cruise was 2–3 °C colder than the ones used for the other cruises. Potentially, unlike every other site, isotope equilibration occurred here, but total equilibration of the added 1 nmol L^{-1} ^{63}Ni with 3–5 nmol L^{-1} Ni would reduce the observed uptake rates 3–5-fold, an effect insufficient to explain the discrepancy. If the diatom-dominated communities in this region grow predominantly on nitrate, this could result in reduced Ni uptake rates, yet the uptake of Ni by diatoms growing on nitrate has not

been studied. Pervasive Fe limitation of phytoplankton communities in the Peru upwelling may also contribute to the regional differences in Ni uptake rates, as discussed in the next section.

4.6. Cell-surface area models of Ni uptake in HNLC and non-HNLC regions

Ni concentrations measured in the surface waters of Peru12 and GOCAL3 were 4-fold higher than the Ni additions, which would seem to be at odds with the observed biological response from the fertilization experiments. In previous reports of trace metal limitation or colimitation in oceanic ecosystems, the dissolved seawater concentrations of the limiting nutrient were always vanishingly low (Crawford et al., 2003; Rue and Bruland, 1995; Saito et al., 2005). The GOCAL3 community was dominated by *Synechococcus*-like cyanobacteria, and free $[\text{Ni}^{2+}]$ less than 100 pmol L^{-1} reduces the growth rates of *Synechococcus* (Dupont et al., 2008a). Therefore, a complexation of greater than 97% of the ambient Ni by organic ligands would result in growth limitation of *Synechococcus*. Chemical measurements of Ni speciation were not conducted, yet the uptake kinetics experiments from GOCAL3 revealed that most if not all of the ambient 3.5 nmol L^{-1} did not equilibrate with the added radioisotope on time scales of less than 6 h (Fig. 4B). If this is due to chelation by ligands, it seems conceivable that the cyanobacteria-dominated community at GOCAL3 is simply limited by low free Ni concentrations. Such an explanation would be at odds with measurements of Ni speciation conducted using electrochemical methods (Saito et al., 2004), but weak ligands might not be detected by a method that uses an exceptionally strong competing ligand like DMG. Certainly, two separate lines of evidence derived from biochemical interrogations of natural phytoplankton communities suggest that the Ni might be complexed by organic ligands.

An alternative explanation for the observed Ni and Ni-urea colimitation at GOCAL3 and Peru12, respectively, involves the kinetics of metal uptake and the membrane space available for transporters. Due to the low concentrations of bioactive metals in seawater, a paradoxically greater number of transporters are necessary to acquire the trace elements compared with the macronutrients C, N, and P, despite the disparity in cellular requirements (Morel et al., 1991). Trace metal uptake by phytoplankton in seawater is under kinetic control; therefore the number of surface transporters (L) required is directly related to the growth rate (μ) and inversely related to the ligand complex formation rate constant (K_f) and the labile concentrations of the metal ($[\text{M}']$ e.g. $[\text{Ni}^{2+}]$) (Hudson and Morel, 1993). The surface area of the cell provides a biophysical limit on the maximum number of transporters (L_{\max}), and trace metal limitation can theoretically occur through a lack of membrane space with transporter proteins. Of the biologically-utilized trace elements, Ni and Fe have the slowest complex formation kinetics and are most likely to result in membrane crowding, though previously each metal was considered in isolation (Morel et al., 1991).

Using the relationships described above and simplified models representative of a cyanobacterial and diatom cell, the relationships between membrane space occupied by transporters and Ni concentrations was examined. Two scenarios were tested: what proportion of the cellular membrane space is required for just Ni transporters over a range of $[\text{Ni}^{2+}]$ (case 1) and how much membrane space is required for both Ni and Fe transporters over a range of $[\text{Ni}^{2+}]$ assuming a constant $[\text{Fe}']$ (case 2). The percent of the outer membrane actually available for transporters is unknown, and while 10% seems a plausible upper limit (Button,

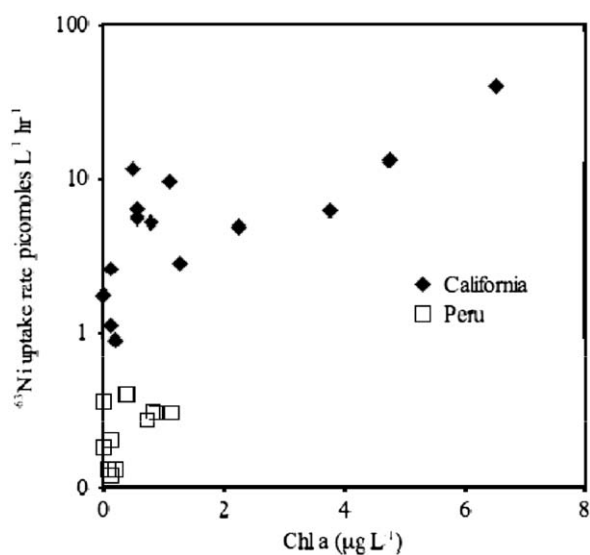


Fig. 6. ^{63}Ni uptake rates measured using 1 nmol L^{-1} ^{63}Ni additions plotted against the observed particulate Chl *a* concentrations.

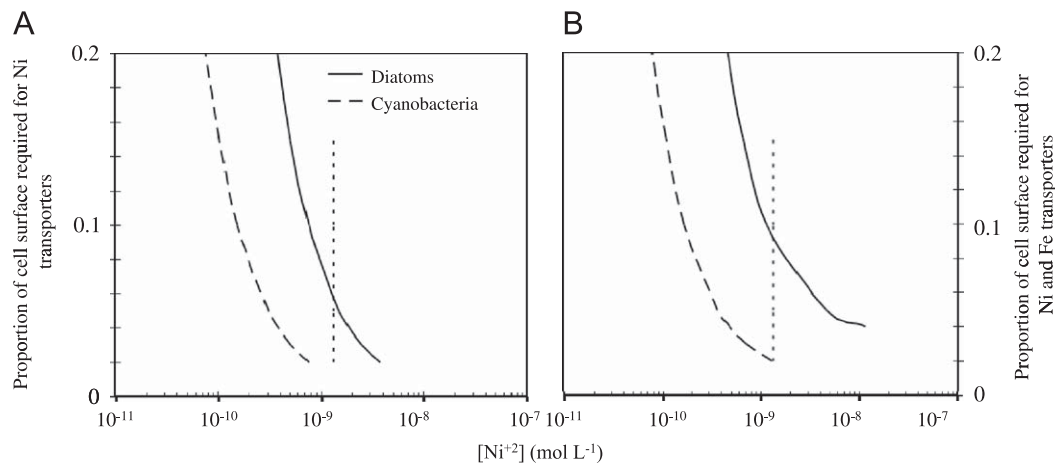


Fig. 7. Ni, Fe, and membrane space requirements in cyanobacteria and diatoms. Shown is the proportion of the cell surface (y-axis) occupied by Ni transporters required by either cyanobacteria or diatoms to grow at specific $[\text{Ni}^{2+}]$ (x-axis). Decreasing Ni concentrations result in an increased proportion of the membrane being devoted to Ni uptake to the point where growth is limited by a lack of membrane space (presumed to be 0.1–0.2). In panel A, Ni is considered in isolation. In panel B, the amount of membrane space required for both Ni and Fe transporters is determined and summed. The models, which are meant to be representative of the natural communities at GOCAL 3 and Peru12, and associated parameters are detailed in Table 4. For reference, the vertical line shows the Ni^{2+} concentrations assuming just inorganic complexation.

Table 4

Equations and parameters for the modeling of cell surface saturation shown in Fig. 7.

Case 1: $[\text{Ni}^{2+}]$ resulting in saturation of 2–20% of the cell surface $[\text{Ni}^{2+}] = \mu Q_{\text{Ni}} K_{\text{f-Ni}}^{-1} L_{\text{sat}}^{-1}$ where $L_{\text{sat}} = 0.02\text{--}0.1$ (cell $r^2 \times$ transporter r^{-2})	
Case 2: $[\text{Ni}^{2+}]$ resulting in saturation of 2–20% of the cell surface when accounting for required Fe transporters $[\text{Ni}^{2+}] = \mu Q_{\text{Ni}} K_{\text{f-Ni}}^{-1} L_{\text{sat}}^{-1}$ $L_{\text{sat}} = 0.02\text{--}0.1$ (cell $r^2 \times$ transporter r^{-2}) $- L_{\text{Fe}}$ $L_{\text{Fe}} = \mu Q_{\text{Fe}} K_{\text{f-Fe}}^{-1} [\text{Fe}']^{-1}$	
GOCAL 3 (cyanobacteria)	Peru 12 (diatoms)
$\mu = 1 \text{ day}^{-1}$	$\mu = 1.5 \text{ day}^{-1}$
$Q_{\text{Ni}} = 10^{-20} \text{ mol cell}^{-1}$	$Q_{\text{Ni}} = 3.3 \times 10^{-18} \text{ mol cell}^{-1}$
$Q_{\text{Fe}} = 4 \times 10^{-19} \text{ mol cell}^{-1}$	$Q_{\text{Fe}} = 5 \times 10^{-18} \text{ mol cell}^{-1}$
$K_{\text{f-Ni}} = 10^5 \text{ L mol}^{-1} \text{ s}^{-1}$	$K_{\text{f-Ni}} = 10^5 \text{ L mol}^{-1} \text{ s}^{-1}$
$K_{\text{f-Fe}} = 2 \times 10^6 \text{ L mol}^{-1} \text{ s}^{-1}$	$K_{\text{f-Fe}} = 2 \times 10^6 \text{ L mol}^{-1} \text{ s}^{-1}$
Cell $r = 0.5 \text{ }\mu\text{m}$	Cell $r = 5.0 \text{ }\mu\text{m}$
Transporter $r = 2.3 \text{ nm}$	Transporter $r = 2.3 \text{ nm}$
$[\text{Fe}'] = 3.67 \text{ nmol L}^{-1}$	$[\text{Fe}'] = 170 \text{ pmol L}^{-1}$

In case 1, the number of transporters (L) required to fill a percentage (2–20%) of the membrane was calculated. Then the Ni concentration that necessitates that number of transporters was calculated. In case two, the number of required Fe transporters was calculated first and assumed to remove part of the membrane available for the placement of Ni transporters.

1998), a range of 2–20% was examined. The oceanic *Synechococcus* sp. WH8102 was chosen to represent the GOCAL3 community, with growth rates and Q_{Ni} being taken from Dupont et al. (2008a). The Fe quotas for the cyanobacteria were calculated from the Fe associated with the cyanobacteria community in the FeCycle experiment, a *Synechococcus*-dominated low-nitrogen site (Strzepek et al., 2005). PERU12 was modeled using the oceanic diatom *Thalassiosira oceanica*, with the Ni quotas from Price and Morel (1991, after scaling for the differences in cell size between *T. weissflogii* and *T. oceanica*) and the Fe quotas from Sunda and Huntsman (1995). It was assumed that the measured total dissolved Fe concentrations (Table 2) represent bioavailable Fe, as has been concluded from culture studies and mesoscale Fe fertilization experiments (Maldonado and Price, 2001; Rue and Bruland, 1997). Naturally, this model will be greatly influenced by the physical size of the transporter, and genomic evidence

suggests that Fe uptake is accomplished by a great diversity of molecular approaches. We purposely chose a small transporter diameter to make the results of this model conservative.

In Fig. 7, the fraction of the cell surface required for Ni (A) and Ni+Fe (B) transporters is plotted against $[\text{Ni}^{2+}]$ concentrations. Decreasing $[\text{Ni}^{2+}]$ results in a greater need for Ni transporters and membrane space, while the accounting for Fe transporters further exacerbates this requirement. This modeling provides some explanation for the results from the fertilization experiments. Examining just Ni transporters and assuming that only 10% of the outer membrane is available for transporters, Ni limitation in cyanobacteria would occur at $[\text{Ni}^{2+}] < 100\text{--}200 \text{ pM}$ while diatoms would be limited at $\sim 750 \text{ pM}$. Owing to the hyperbolic relationship of the trace metal concentrations and transporter requirements, an addition of 750 pmol L^{-1} total Ni reduces the required membrane space to a near minimum (Fig. 7A). For diatom-dominated community exposed to low Fe, almost 10% (the maximum) of the outer membrane is required simply to acquire Ni and Fe (Fig. 7B), even in the absence of chelation by ligands. Again, an addition of 750 pmol L^{-1} Ni would reduce this percentage greatly (Table 4).

5. Conclusions

Two distinct scenarios were observed where Ni affected the growth and biomass of natural phytoplankton communities. The observation of both biochemically dependent and independent Ni–urea colimitation is consistent with culture studies linking the biochemical role of Ni to growth requirements and genomic contents, Ni uptake measurements conducted in parallel, and theoretical models of the transporter requirements. Naturally, further integrated fertilization and uptake kinetics experiments in biogeochemically distinct regimes are required. Future incubation experiments certainly should incorporate additional biomass measurements (particular organic carbon, microscopy), but also should focus on the effects of Ni and urea additions on physiological parameters, particularly primary production, Ni and urea uptake rates, and active fluorescence.

While the Ni limitation in Peru was artificially induced by the addition of urea to a community likely growing on nitrate, the result has implications for the physiological state of the community.

Phytoplankton confronted with multiple nutrient limitations will optimize transporter ratios to best satisfy moderately plastic cellular requirements (Smith and Yamanaka, 2007), though there will be biochemical ramifications from the reduced uptake of certain nutrients. In the case of the Peru community, low Fe concentrations may force the diatoms to sacrifice urease activity to reduce Ni requirements and the attendant need for Ni transporters, which is consistent with the exceptionally low observed Ni uptake rates in Peru (Fig. 7). Diatoms have a complete urea cycle, which may be important in the intracellular recycling of nitrogen generated by photorespiration (Allen et al., 2006). Within this cycle, urease may be required to recover NH_4^+ from arginase-produced urea (Quintero et al., 2000), which is otherwise lost. Therefore, a consequence of low Fe concentrations may be an inefficient recycling of nitrogen in diatoms, resulting in heightened rates of organic nitrogen release, a ubiquitous phenomenon in the marine environment (Bronk et al., 1994). This organic nitrogen, urea included, would likely be available for uptake by bacteria and picoplankton that, due to their smaller cell size, are less likely to be Ni–Fe–N colimited.

While large abrupt inputs of urea to an oceanic environment are unlikely to occur, except in regions affected by agricultural run-off (Glibert et al., 2006), the Ni–urea colimitation observed in Peru nevertheless suggests that Fe-limited large phytoplankton may have inefficient internal N-recycling. Measurements of community urease activity in different regimes would test if HNLC conditions result in a restructuring of urea and Ni metabolism. Additionally, biomass-normalized Ni uptake rates in HNLC waters should increase dramatically following the addition of Fe if the transporter modeling in Fig. 7 is correct. Alternatively, the addition of Fe may allow access to NO_3^- , reducing the need for urease and Ni. Finally, coupling the determination of Ni uptake kinetics and isotope dilution with more traditional chemical methods of Ni speciation measurements would provide insight to the biological relevance of the detection window of the chemical methods.

Acknowledgements

This work was greatly facilitated by the crews and science parties of the R/V *New Horizon* and R/V *Knorr*. Specifically, B. Hopkinson, A.L. King, D. Chappelle, J. W. Moffett, T. Goepfert, B. Popp, R. Wallsgrove, R. Palomares, and V. Tai helped with the sampling, S. Reynolds helped with the pigment measurements, and A. L. King provided several Fe measurements. The manuscript was improved by suggestions from two anonymous reviewers. Ship time and supplies for the coastal California studies was funded by the National Science Foundation California Current Ecosystem-Long Term Ecological Research Grant (OCE-0417616). K. N. B. was supported by a Scripps Institution of Oceanography Earth Sciences Postdoctoral Fellowship and C. L. D. was supported by a National Defense Science and Engineering Graduate Research Fellowship. This work was partially funded by grants from the NSF-DOE funded Princeton Center for Environmental Bioinorganic Chemistry to C. L. D.

References

- Allen, A.E., Vardi, A., Bowler, C., 2006. An ecological and evolutionary context for integrated nitrogen metabolism and related signaling pathways in marine diatoms. *Current Opinion in Plant Biology* 9 (3), 264–273.
- Arrigo, K.R., 2005. Marine microorganisms and global nutrient cycles. *Nature* 437, 349–355.
- Barondeau, D.P., Kassman, C.J., Bruns, C.K., Tainer, J.A., Getzoff, E.D., 2004. Nickel superoxide dismutase structure and mechanism. *Biochemistry* 43, 8038–8047.
- Baumgartner, T.R., Ferreira-Bartrina, V., Moreno-Hentz, P., 1991. Varve formation in the central Gulf of California: a reconsideration of the origin of the dark laminae from the 20th century varve record. In: Dauphin, J.P., Simoneit, B. (Eds.), *The Gulf and Peninsular Province of the Californias*. American Association of Petroleum Geologists Memoir, pp. 617–635.
- Bedworth, W.W., Sedlak, D.L., 1999. Sources and environmental fate of strongly complexed nickel in estuarine waters: the role of ethylenediaminetetraacetate. *Environmental Science and Technology* 33, 926–931.
- Bronk, D.A., Glibert, P.M., Ward, B.B., 1994. Nitrogen uptake, dissolved organic nitrogen release and new production. *Science* 265, 1843–1846.
- Bruland, K.W., Rue, E.L., Smith, G.J., DiTullio, G.R., 2005. Iron, macronutrients and diatom blooms in the Peru upwelling regime: brown and blue waters of Peru. *Marine Chemistry* 93, 81–103.
- Buck, K.N., Lohan, M.C., Berger, C.J.M., Bruland, K.W., 2007. Dissolved iron speciation in two distinct river plumes and an estuary: implications for riverine iron supply. *Limnology and Oceanography* 52 (2), 843–855.
- Button, D.K., 1998. Nutrient uptake by microorganisms according to kinetic parameters from theory as related to cryoarchitecture. *Microbiology and Molecular Biology Reviews* 62 (3), 636–645.
- Cho, B.C., Azam, F., 1995. Urea decomposition by bacteria in the Southern California Bight and its implications for the mesopelagic nitrogen cycle. *Marine Ecology-Progress Series* 122, 21–26.
- Collier, J.L., Brahmsha, B., Palenik, B., 1999. The marine cyanobacterium *Synechococcus* sp. WH 7805 requires urease (urea amidohydrolase, EC 3.5.1.5) to utilize urea as a nitrogen source: molecular-genetic and biochemical analysis of the enzyme. *Microbiology* 145, 447–459.
- Collier, J.L., Palenik, B., 2003. Phycoerythrin-containing picoplankton in the Southern California Bight. *Deep-Sea Research II* 50, 2405–2422.
- Crawford, D.W., et al., 2003. Influence of zinc and iron enrichments on phytoplankton growth in the northeastern subarctic Pacific. *Limnology and Oceanography* 48 (4), 1583–1600.
- Dixon, J.L., et al., 2006. Cadmium uptake by marine micro-organisms in the English Channel and Celtic Seas. *Aquatic Microbial Ecology* 44, 31–43.
- Donat, J., Lao, K., Bruland, K., 1994. Speciation of dissolved copper and nickel in South San Francisco Bay: a multi-method approach. *Analytica Chimica Acta* 284, 547–571.
- Donat, J.R., Bruland, K.W., 1988. Direct determination of dissolved cobalt and nickel in seawater by differential pulse cathodic stripping voltammetry preceded by adsorptive collection of cyclohexane-1, 2-dione dioxime complexes. *Analytical Chemistry* 60, 240–244.
- Dupont, C.L., Barbeau, K., Palenik, B., 2008a. Ni uptake and limitation in marine *Synechococcus* strains. *Applied and Environmental Microbiology* 74 (1), 23–31.
- Dupont, C.L., Neupane, K.P., Shearer, J., Palenik, B., 2008b. Diversity, function, and evolution of genes coding for putative Ni-containing superoxide dismutases. *Environmental Microbiology* 10 (7), 1831–1843.
- Dyhrman, S.T., Anderson, D.M., 2003. Urease activity in cultures and field populations of the toxic dinoflagellate *Alexandrium*. *Limnology and Oceanography* 48 (2), 647–655.
- Fridovich, I., 1997. Superoxide anion radical (O_2^-), superoxide dismutases, and related matters. *Journal of Biological Chemistry* 272 (30), 18515–18517.
- Glibert, P.M., Harrison, J., Heil, C.A., Seitzinger, S., 2006. Escalating worldwide use of urea – a global change contributing to coastal eutrophication. *Biogeochemistry* 77, 441–463.
- Goericke, R., Montoya, J.P., 1998. Estimating the contribution of microalgal taxa to chlorophyll *a* in the field—variations of pigment ratios under nutrient- and light-limited growth. *Marine Ecology-Progress Series* 169, 97–112.
- Hallam, S.J., et al., 2006. Pathways of carbon assimilation and ammonia oxidation suggested by environmental genomic analyses of marine *Crenarchaeota*. *PLoS Biology* 4 (4), e95.
- Hausinger, R.P., 2004. Metabolic versatility of prokaryotes for urea decomposition. *Journal of Bacteriology* 186 (9), 2520–2522.
- Healey, F.P., 1980. Slope of the Monod equation as an indicator of advantage in nutrient competition. *Microbial Ecology* 5 (4), 281–286.
- Heil, C.A., Revilla, M., Glibert, P.M., Murasko, S., 2007. Nutrient quality drives differential phytoplankton community composition on the southwest Florida shelf. *Limnology and Oceanography* 52 (3), 1067–1078.
- Hudson, R.J.M., Morel, F.M.M., 1993. Trace metal transport by marine microorganisms: implications of metal coordination kinetics. *Deep-Sea Research* 40, 129–150.
- Huerta-Diaz, M.A., Leon-Chavira, F., Lares, M.L., Chee-Barragan, A., Siqueiros-Valencia, A., 2007. Iron, manganese and trace metal concentrations in seaweeds from the central west coast of the Gulf of California. *Applied Geochemistry* 22, 1380–1392.
- Johnson, K.S., et al., 2007. The SAFE iron intercomparison cruise: an international collaboration. *EOS* 88, 131–132.
- Klotz, M.G., et al., 2007. Complete genome sequence of the marine, chemolithoautotrophic, ammonia-oxidizing bacterium *Nitrosococcus oceanus* ATCC19707. *Applied and Environmental Microbiology* 72 (9), 6299–6315.
- Koroleff, F., 1983. Determination of Ammonia, *Methods of Seawater Analysis*. Verlag Chemie, Weinheim, pp. 150–157.
- Kszos, L.A., Stewart, A.J., Taylor, P.A., 1992. An evaluation of nickel toxicity to *Ceriodaphnia dubia* and *Daphnia magna* in a contaminated stream and in laboratory tests. *Environmental Toxicology and Chemistry* 11 (7), 1001–1012.
- Mackey, D.J., O'Sullivan, J.E., Watson, R.J., Dal Pont, G., 2002. Trace metals in the Western Pacific: temporal and spatial variability in the concentrations of Cd, Cu, Mn, and Ni. *Deep-Sea Research I* 49 (12), 2241–2259.
- Maldonado, M.T., Price, N.M., 2001. Reduction and transport of organically bound iron by *Thalassiosira oceanica* (Bacillariophyceae). *Journal of Phycology* 37, 298–309.

- Maldonado, M.T., Boyd, P.W., LaRoche, J., Strzepek, R., Waite, A., Bowie, A.R., Croot, P.L., Frew, R.D., Price, N.M., 2001. Iron uptake and physiological response of phytoplankton during a mesoscale Southern Ocean iron enrichment. *Limnology and oceanography* 46, 1802–1808.
- Morel, F.M.M., Hudson, R.J.M., Price, N.M., 1991. Limitation of productivity by trace metals in the sea. *Limnology and Oceanography* 36, 1742–1755.
- Morel, F.M.M., Milligan, A.J., Saito, M.A., 2003. Marine bioinorganic chemistry: the role of trace metals in the oceanic cycles of major nutrients. In: Elderfield, H., Holland, H.D., Turekian, K.K. (Eds.), *Treatise on Geochemistry: The Oceans and Marine Geochemistry*. Elsevier, pp. 113–143.
- Oliveria, L., Antia, N.J., 1986. Nickel ion requirements for autotrophic growth of several marine microalgae with urea serving as nitrogen source. *Canadian Journal of Fisheries and Aquatic Sciences* 43, 2427–2433.
- Palenik, B., Henson, S., 1997. The use of amides and other organic nitrogen sources by the coccolithophorid *Emiliania huxleyi*. *Limnology and Oceanography* 42, 1544–1551.
- Price, N.M., Anderson, L.F., Morel, F.M.M., 1991. Iron and nitrogen nutrition of equatorial Pacific plankton. *Deep-Sea Research I* 38, 1361–1378.
- Price, N.M., et al., 1988/1989. Preparation and chemistry of the artificial algal culture medium Aquil. *Biological Oceanography* 6, 443–461.
- Price, N.M., Morel, F.M.M., 1991. Colimitation of phytoplankton growth by nickel and nitrogen. *Limnology and Oceanography* 36, 1071–1077.
- Quintero, M.J., Muro-Pastor, A.M., Herrero, A., Flores, E., 2000. Arginine catabolism in the cyanobacterium *Synechocystis* sp. strain PCC6803 involves the urea cycle and arginase pathway. *Journal of Bacteriology* 182 (4), 1008–1015.
- Revilla, M., Alexander, J., Glibert, P.M., 2005. Urea analysis in coastal waters: comparison of enzymatic and direct methods. *Limnology and Oceanography: Methods* 3, 290–299.
- Rue, E.L., Bruland, K.W., 1995. Complexation of iron(III) by natural organic ligands in the Central North Pacific as determined by a new competitive ligand equilibration/adsorptive cathodic stripping voltammetric method. *Marine Chemistry* 50, 117–138.
- Rue, E.L., Bruland, K.W., 1997. The role of organic complexation on ambient iron chemistry in the equatorial Pacific Ocean and the response of a mesoscale iron addition experiment. *Limnology and Oceanography* 42, 901–910.
- Saito, M.A., Goepfert, T.J., Ritt, J.T., 2008. Some thoughts on the concept of colimitation: three definitions and the importance of bioavailability. *Limnology and Oceanography* 53 (1), 276–290.
- Saito, M.A., Moffett, J.W., DiTullio, G.R., 2004. Cobalt and nickel in the Peru upwelling region: a major flux of labile cobalt utilized as a micronutrient. *Global Biogeochemical Cycles* 18, 4030–4044.
- Saito, M.A., Rocap, G., Moffett, J.W., 2005. Production of cobalt binding ligands in a *Synechococcus* feature at the Costa Rica upwelling dome. *Limnology and Oceanography* 50 (1), 279–290.
- Schmidt, M.A., Hutchins, D.A., 1999. Size-fractionated biological iron and carbon uptake along a coastal to offshore transect in the NE Pacific. *Deep-Sea Research II* 46 (11–12), 2487–2503.
- Slater, F.R., Boyle, E.A., Edmond, J.M., 1976. On the marine geochemistry of nickel. *Earth and Planetary Science Letters* 31, 119–128.
- Smith, W.L., Yamanaka, Y., 2007. Optimization-based model of multnutrient uptake kinetics. *Limnology and Oceanography* 52 (4), 1545–1558.
- Strzepek, R.F., et al., 2005. Spinning the “ferrous wheel”: the importance of the microbial community in an iron budget during the FeCycle experiment. *Global Biogeochemical Cycles* 19, GB4S26, doi:10.1029/2005GB002490.
- Sunda, W.G., Huntsman, S.A., 1992. Feedback interactions between zinc and phytoplankton in seawater. *Limnology and Oceanography* 37 (1), 25–40.
- Sunda, W.G., Huntsman, S.A., 1995. Iron uptake and growth limitation in oceanic and coastal phytoplankton. *Marine Chemistry* 50, 189–206.
- Thunell, R.C., 1998. Seasonal and annual variability in particle fluxes in the Gulf of California: a response to climate forcing. *Deep-Sea Research II* 45, 2059–2083.
- Wafar, M.V.M., Lecorre, P., Lhelguen, S., 1995. F-ratios calculated with and without urea uptake in nitrogen uptake by phytoplankton. *Deep-Sea Research I* 42 (9), 1669–1674.
- White, A.E., Pahl, F.G., Letelier, R.M., Popp, B.N., 2007. Summer surface waters in the Gulf of California: prime habitat for biological N₂ fixation. *Global Biogeochemical Cycles* 21, GB2017.
- Wyman, M., Gregory, R.P.F., 1985. Novel role for phycoerythrin in a marine cyanobacterium, *Synechococcus* strain DC2. *Science* 230 (4727), 818–820.